SPAN LENGTH INFLUENCE ON DYNAMIC RESPONSE OF SELECTED BRIDGE UNDER HIGH-SPEED TRAIN

Piotr Szurgott, Paweł Bernacki

Military University of Technology
Department of Mechanics and Applied Computer Science
Gen. Sylwestra Kaliskiego Street 2, 00-908 Warsaw, Poland
tel.: +48 22 6837272, fax: +48 22 6839355
e-mail: pszurgott@wat.edu.pl

Abstract

The paper presents a methodology of finite element (FE) modelling and simulation of the bridge – track – moving high-speed train system using CAE systems. Two composite (reinforce-concrete – steel) bridges were considered. The span length was equal to 15 and 21 meters, respectively. Bridges selected for the study belong to the proposed series of bridges with the span length of 15 to 27 meters stepped by 3 meters. Full symmetry of the bridges was assumed. RC platform was homogenized since the rebars were distributed quasi-uniformly in the specified platform sections. The FE model of a bridge superstructure consisted of 4-node shell elements (main beams) and 8-node 48 DOF solid elements (reinforced concrete platform). RAIL_TRACK and RAIL_TRAIN LS-DYNA's modules were applied for simulating the moving train – track interaction. Ballasted track with the rectilinear rail-line axis was taken into consideration. German ICE-3 train running at velocity of 200–300 km/h was selected as a representative for the study. All mass components of the train FE model were treated as rigid bodies. Symmetric vibrations of the train units were assumed with respect to the main longitudinal vertical plane of symmetry of the system. Nodal displacement and longitudinal normal stress in shell elements were registered during the FE analysis. The results were depicted in the form of time histories for selected velocities. In addition, extreme values of vertical deflections and normal stress were compiled and presented a function of train velocity. It allowed to assess the dynamic response of the bridge depending on its span length. Contours of resultant displacement for the RC platform was also presented.

Keywords: *railway bridge, composite bridge, ballasted track, high-speed train, modelling and simulation*

1. Introduction

Nowadays, complexity of the bridge – track – train system (BTT system) makes its modelling a challenge for scientists. Nonlinear models are described with a huge number of parameters. Many of these parameters, regarding fastening systems, ballast, subsoil layers, suspensions of the railway vehicles, etc., are difficult for identification. Therefore, some of them are mostly estimated. Producers and research institutions involved in modern high-speed trains do not bring to light structural details, values of parameters or their research results. Above mentioned inconveniences make precise prediction of dynamic response of bridges under moving trains very difficult.

At present, it can be observe various numerical approaches to dynamics of bridges generally. Commercial CAE systems are more and more often used in such problems. Modelled systems are generally three-dimensional, however they may be considered as simplified ones due to the vertical longitudinal plane of symmetry. Such approach was proposed by Authors in current study.

A methodology of the FE modelling and simulation of the BTT system presented in this paper was developed with the use of commercial CAE systems. It is related to the reinforce-concrete – steel bridge, ballasted track and high-speed train. Altair HyperMesh, LS-DYNA and LS-PrePost software was applied in the methodology. Author's approach is based on homogenization of the bridge RC platform, RAIL_TRACK and RAIL_TRAIN modules for simulating the train – track interaction, non-linear modelling of rail fasteners and ballast, application of constrained joints and discrete springs and dampers for modelling suspensions in railway vehicles.

2. Study objects

Series of bridges, according to [6], was proposed for the study. Two representatives – 15- (CB15 code) and 21-meter span (CB21 code) – were taken into consideration. Schemes of the considered bridges are depicted in Fig. 1. Cross-section of the reinforce-concrete platform is the same for all bridges in series. Main differences appear in the steel main beams. Although the spacing is the same (2.5 m), the vertical dimensions of bottom flanges and the web height are differ depending on the bridge length. Each main beam includes top and bottom flanges, web and vertical ribs every 1.5 m welded to the web on both sides. Each bottom flange is reinforced with two additional steel plates. Transverse bracing system between main beams was omitted in simulation.

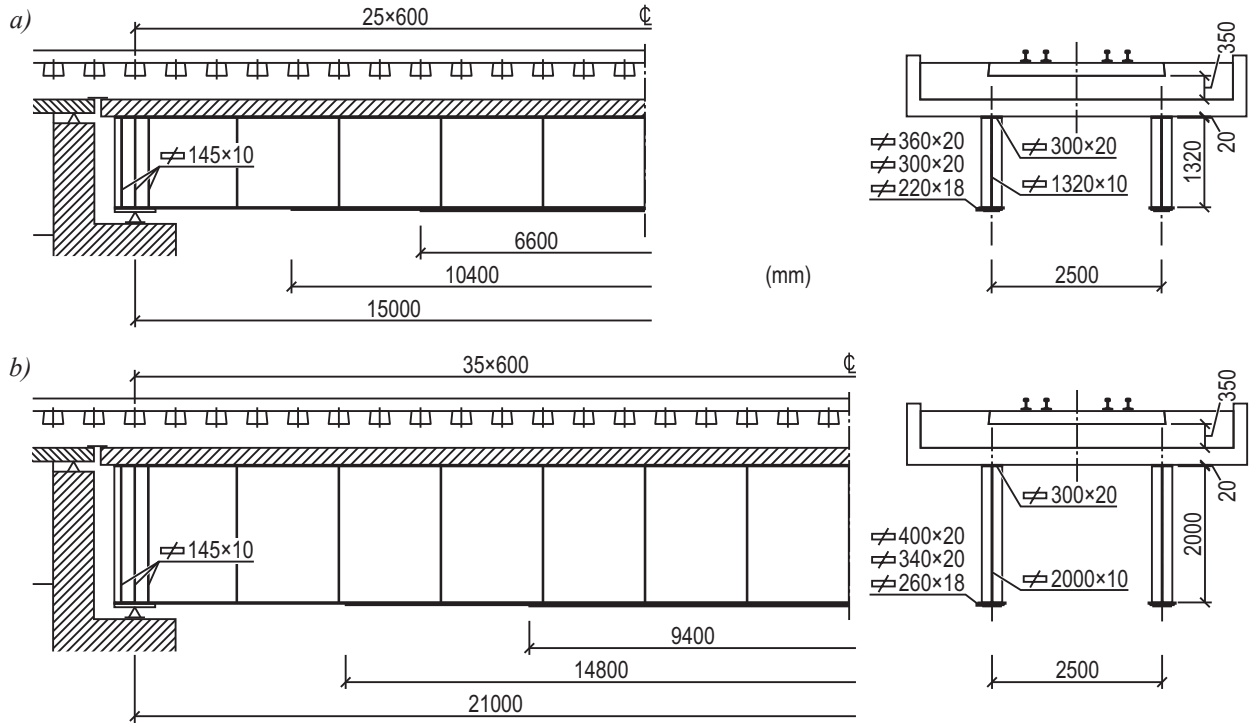

Fig. 1. Schemes of the considered bridges in the longitudinal and the cross-section: CB15 (a) and CB21 (b). Selected dimensions of the steel components are presented

The reinforcement of the platform is also different for the bridges under consideration. Both platforms include similar sections A, B_1, B_2, B_3, C and D, presented in Fig. 2. Respective sections have the same system of rebars regardless of the bridge length but the longitudinal dimensions of each section – especially B_1, B_2 and B_3 – are proportional to the span length. Reinforcement of the RC platform was distributed quasi-uniformly in the specified platform sections. Therefore, the platform was homogenized [5] for numerical modelling. Such approach allowed to reflect the RC platform by linear viscoelastic orthotropic material described by 3 Young's moduli, 3 Poisson's ratios, and 3 shear moduli in each subarea.

The ballasted track was taken into consideration. The track structure consists of UIC 60 main rails, B320 sleepers with Vossloh 300-1 fastening system, and the first class ballast. Additional side rails UIC 60 and SB3 fasteners were applied in approach and the bridge zones. The embankment in the approach zones contains cement-stabilized subsoil, while the approach zones an upper 0.2 m thick sand-gravel mix layer was used. The ballast layer was 0.35 m thick under sleepers. The approach slabs before and behind the bridge were applied.

German ICE-3 high-speed train running at velocity of 200–300 km/h over the bridge was selected for the study. Its total weight is distributed evenly across the entire trainset, therefore the axle load was reduced to 16 tons (about 160 kN). A scheme of the ICE-3 trainset is depicted in Fig. 3.

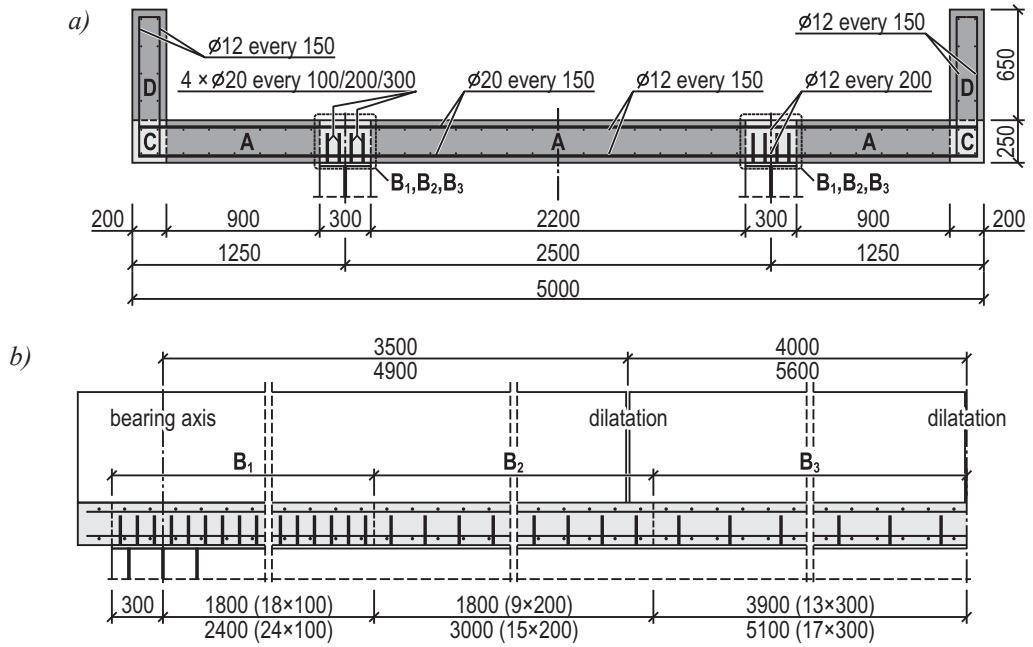

Fig. 2. Cross-section (a) and the longitudinal section (b) of the RC platform including specified sections. Dimensions for both span length variants are given, respectively. Selected reinforcement elements are presented

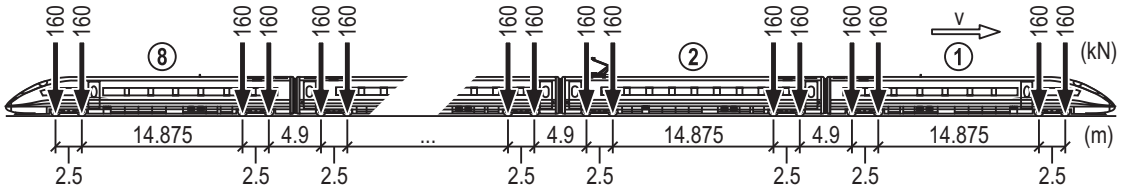

Fig. 3. A scheme of the ICE-3 high-speed trainset [3]

3. Numerical modelling and simulation

The FE model of the bridge superstructure (Fig. 4) was developed in Altair HyperMesh software. 4-node shell elements were used for the main beams modelling, whereas the 8-node 48 DOF solid elements – for the reinforced concrete platform divided into orthotropic parts. Roller bearings and pivot bearings on the bridge abutments were reflected by respective constraints.

The main and side rails were considered as prismatic beams deformable in flexure and shear, made of linearly viscoelastic material. Layers of the embankment were modelled as a linearly viscoelastic material continuum. The embankment was reflected approximately by a rectangular prism with unmovable side and bottom boundary surfaces and meshed using 8-node 24 DOF solid elements. Sleepers were modelled as elastic beams vibrating only vertically using finite beam elements and respective constraints. Rail fasteners were simulated using massless 1-D discrete spring and damper elements. The ballast layer has been divided into cubicoid columns in coincidence with FE mesh of the parts under the ballast. Each ballast column was reflected by a vertical set of nonlinear spring and damper elements. The lumped mass distribution for the ballast was put into the bottom set of the nodal points contacting the platform slab and the top subsoil layers. Values of geometrical and mechanical parameters of the ballasted track components were extracted from [4, 7, 9, 10], and provided in Tab. 1. FE model of the bridge and the approach zones in shown in Fig. 4. Physical model of the track, including spring and damper elements, is also depicted in Fig. 4.

RAIL_TRACK and RAIL_TRAIN modules available in LS-DYNA were applied for approximate modelling the train – track interaction without simulation of wheels' rotation [2]. Modelling of the ICE-3 trainset was performed in LS-PrePost software. It was assumed that vibrations of the train units are symmetric with respect to the main longitudinal vertical plane of symmetry. A numerical

Tab. 1. Values of the geometrical and mechanical parameters of the ballasted track components [4, 7, 9, 10]. Values provided in one of the consistent set of units recommended in LS-DYNA [2]. Selected parameters of the track correspond to the symbols in physical model depicted in Fig. 4

Component	Parameter, Symbol, Unit	Value
UIC60 rail	principal geometric moment of inertia, I_y (mm^4)	$30.383 \cdot 10^6$
	cross-section area, A (mm^2)	7,670
	mass density, ρ (Mg/mm^3)	$7.85 \cdot 10^{-9}$
	Young's modulus, E (MPa)	210,000
	Poisson's ratio, ν (–)	0.30
Vossloh 300-1 fastener	static stiffness at compressing for load 0–18 kN, k_{f1} (N/mm)	17,000
	static stiffness at compressing (for load 18–53 kN), k_{f2} (N/mm)	30,000
	static stiffness at stretching for load < 0, k_{f3} (N/mm)	3,000
	equivalent viscous damping coefficient, c_f (N s/mm)	2.5
SB3 fastener	static stiffness at compressing for load 0–18 kN, k_{f1} (N/mm)	50,000
	static stiffness at compressing (for load 18–53 kN), k_{f2} (N/mm)	100,000
	static stiffness at stretching for load < 0, k_{f3} (N/mm)	3,000
	equivalent viscous damping coefficient, c_f (N s/mm)	4.2
B 320 sleeper	mass (including fasteners), m_s (Mg)	0.366
ballast	mass density, ρ (Mg/mm^3)	$2.00 \cdot 10^{-9}$
	summer-time static stiffness at compressing, k_{bs} (N/mm)	60 000
	summer-time static stiffness at braking away, k_{bs0} (N/mm)	0
	equivalent viscous damping coefficient, c_{bs} (N s/mm)	14.0
cement-stabilized subsoil	mass density, ρ (Mg/mm^3)	$2.265 \cdot 10^{-9}$
	Young's modulus, E (MPa)	325
	Poisson's ratio, ν (–)	0.20
sand-gravel mix layer	mass density, ρ (Mg/mm^3)	$1.90 \cdot 10^{-9}$
	Young's modulus, E (MPa)	150
	Poisson's ratio, ν (–)	0.20
subsoil embankment	mass density, ρ (Mg/mm^3)	$1.80 \cdot 10^{-9}$
	Young's modulus, E (MPa)	82
	Poisson's ratio, ν (–)	0.20

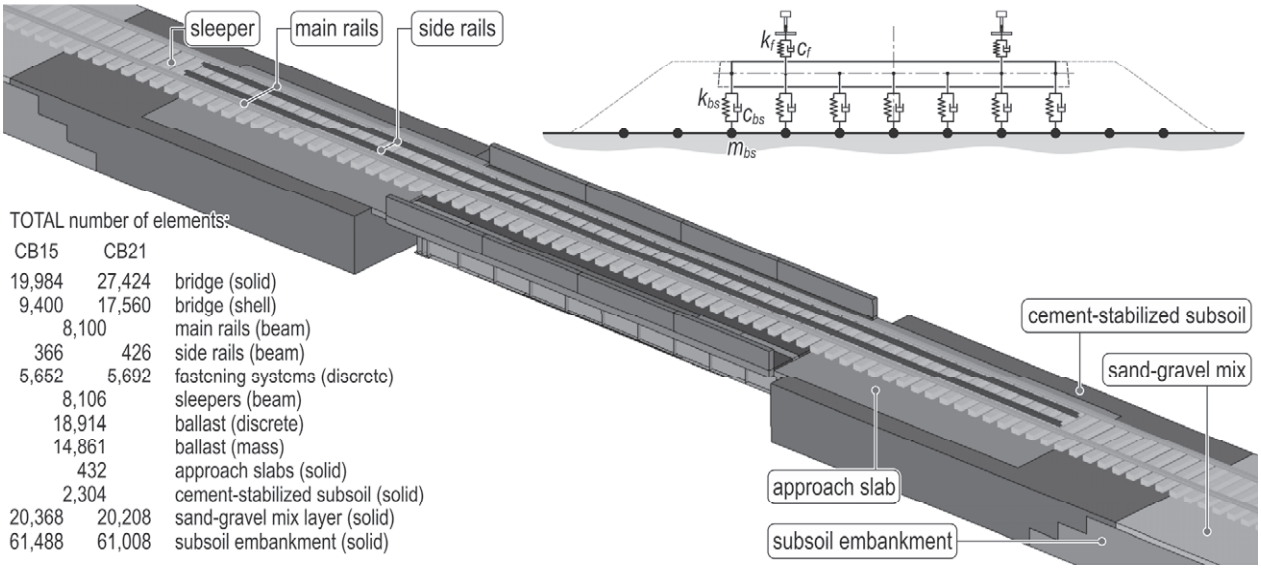

Fig. 4. FE model of the bridge and the track in the approach zone. Main components of the track model are shown. Total number of FE elements is provided. Cross-section of the physical model of the track is presented

model of the train consists of the following components: carbodies, bogie frames, wheel sets – treated as rigid bodies – and vertical massless discrete linear viscoelastic elements reflecting the primary and secondary suspension systems. Respective constraints were put into the system using translational and rotational elements [2]. A side-view scheme of the model of the train unit is shown in Fig. 8. Values of mechanical parameters of the ICE-3 train units were determined according to [1, 8, 11], and provided in Tab. 2.

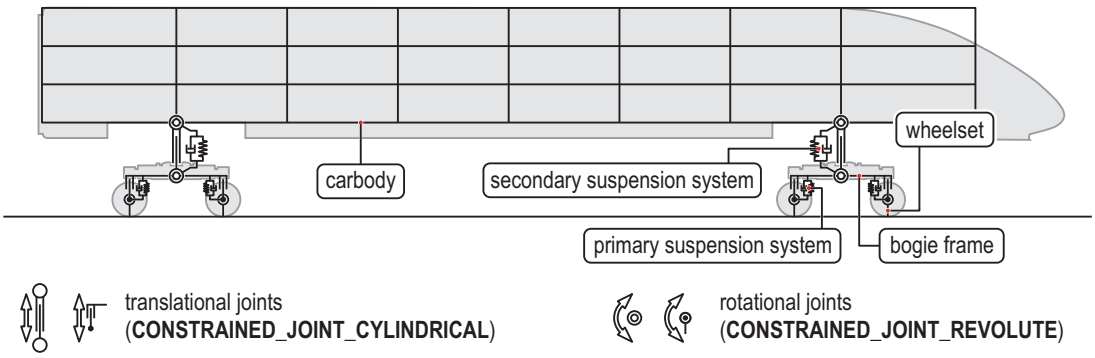

Fig. 5. Side-view scheme of the FE model of the ICE-3 train unit. Components of the model and respective constrained joints are presented

Tab. 2. Values of mechanical parameters of the ICE-3 trainset [1, 8, 11]. Values provided in one of the consistent set of units recommended in LS-DYNA [2]

Parameter, Symbol, Unit	Carriage No. 1, 3, 6 ,8	Carriage No. 2, 4, 5 ,7
mass of the carbody, m_b (Mg)	45.6	49.0
mass of the bogie frame[1)], m_f, (Mg)	4.4	2.7
mass of the wheelset[2)], m_w (Mg)	2.4	2.4
central moment of inertia for the carbody, I_y^b (Mg·mm^2)	$2.397 \cdot 10^9$	$2.576 \cdot 10^9$
central moment of inertia for the bogie frame, I_y^f (Mg·mm^2)	$5.420 \cdot 10^6$	$3.330 \cdot 10^6$
total equivalent vertical stiffness per axle, k_1 (N/mm)	1,124	690
total equivalent vertical damping per axle, c_1 (N·s/mm)	8.8	5.4
total equivalent vertical stiffness per bogie, k_2 (N/mm)	561	603
total equivalent vertical damping per bogie, c_2 (N·s/mm)	27	29
[1)] including bogie frame, bolster, motors, transmissions, joints, pivot etc.		
[2)] including all unsprung masses such as axle boxes, break discs, bearings, etc.		

A set of vertical forces was put in the wheel – rail contact points. Force was increasing from zero up to the value of static axle load according to the formula:

$$P(t) = \frac{P_0}{2}\left(1 - \cos\frac{\pi t}{t_0}\right), \tag{1}$$

where P_0 is static load of a single wheel on the rail head and t_0 is time of increasing of the static load up to the full value, $t_0 = 2$ sec ($0 \le t \le 2$ sec).

4. Results of the FE analysis

Nodal displacement and longitudinal normal stress in shell elements were registered during the FE analysis. The results are presented in the form of time histories for each above mentioned value. Selected measurement points and elements in the midspan are following:

– D1 – bottom flange of the main beam in the web plane,

– S1 – bottom flange of the main beam,
– S2 – top flange of the main beam.

Simulation of dynamic behaviour of the BTT system was carried out for service velocities 200–300 km/h stepped by 10 km/h or — in selected cases — 5 km/h. Extreme values of vertical deflections and longitudinal normal stresses are depicted in Fig. 6. It can be seen that registered values reach a peak for both span length of the bridge. However, it is more noticeable for a shorter span. So-called resonant velocities equal about 215 km/h for CB15 and about 260 km/h for CB21.

Averaged values of deflection are higher for the longer bridge but disparity between peak and the minimum value are smaller. For the shorter bridge an opposite effect is observed. Longitudinal tension stress reach similar values, about 23 MPa, in both cases for velocities beyond the range close to the resonant velocity.

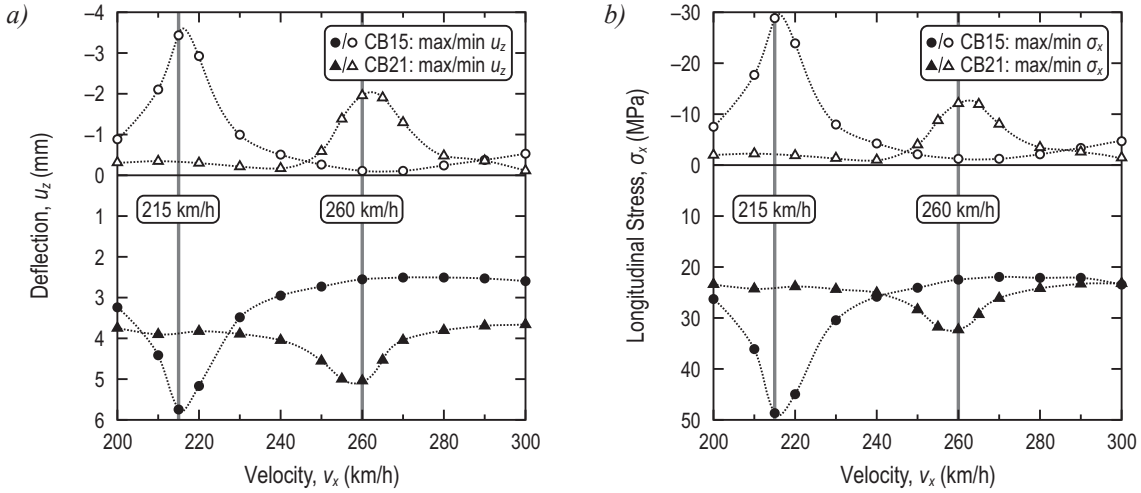

Fig. 6. Extreme values of vertical deflections (a) and longitudinal normal stresses (b) for selected service velocities. The results correspond to the bridge with the span length of 15 m and 21 m

Figure 7 shows time histories of the bridge deflection. Time histories of the longitudinal normal stresses are depicted in Fig. 8 (CB15) and Fig. 9 (CB21) for the maximum velocity of 300 km/h, and for the respective resonant velocities. Time histories are different for both cases and it is strongly related with the span length. Amplitude of the vibration of the shorter bridge is higher. The longitudinal stress values oscillate between 0 and 23 MPa for the CB21 bridge, and between –5 and 22 MPa for the CB15.

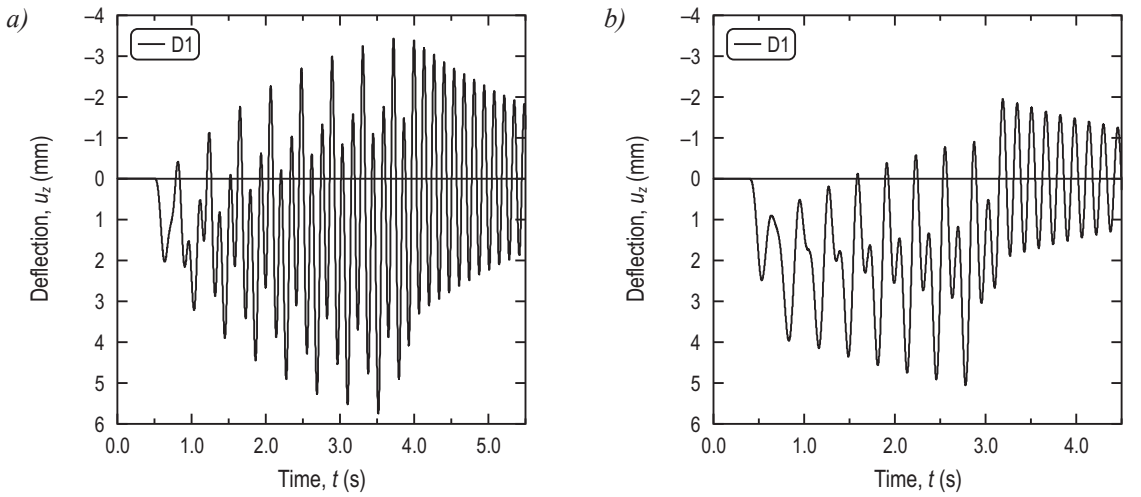

Fig. 7. Time histories of the bridge deflection for the resonant velocities. The results correspond to the CB15 (a) and CB21 (b) bridge

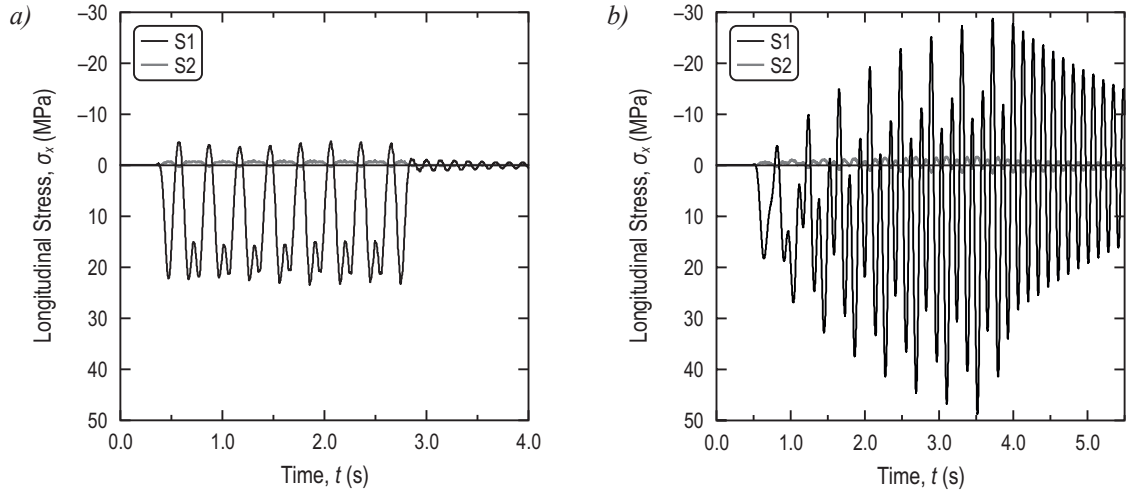

Fig. 8. Time histories of longitudinal normal stresses for the maximum velocity of 300 km/h (a) and for the resonant velocity of 215 km/h (b). The results correspond to the CB15 bridge

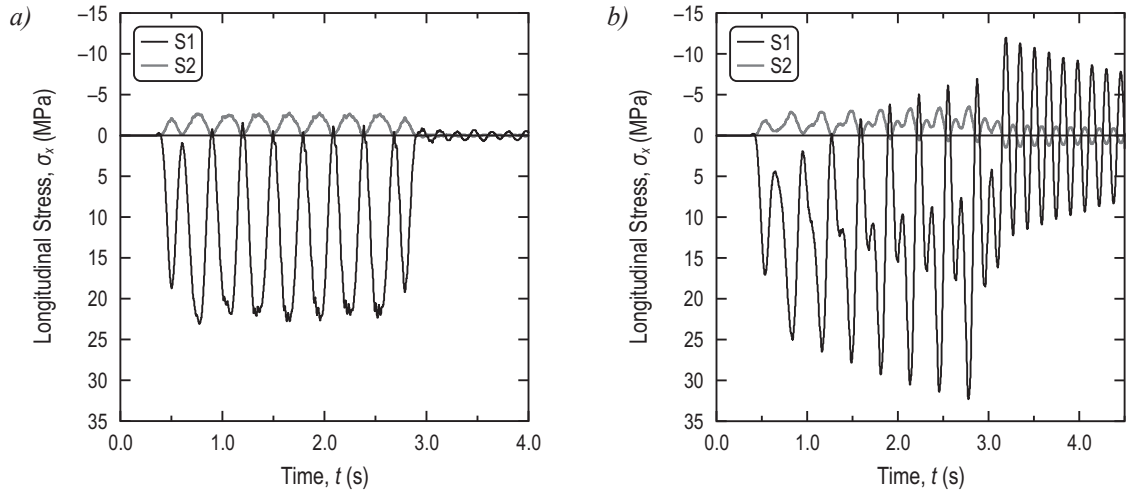

Fig. 9. Time histories of longitudinal normal stresses for the maximum velocity of 300 km/h (a) and for the resonant velocity of 260 km/h (b). The results correspond to the CB21 bridge

Contours of resultant displacement for the RC platform for selected moment of time are depicted in Fig. 10. The scale coefficient 100× for displacements of presented component was applied.

5. Summary and conclusion

The study develops FE modelling and simulation of the bridge – track – train system. Series of bridges was selected for the study. Selected results were presented for two representative bridges, CB15 and CB21, hence the conclusions cannot be generalized for the whole series. Simulation of dynamic behaviour of the BTT system was carried out for the range of velocities between 200 to 300 km/h. One resonant velocity was noticed for each case. It equals about 215 km/h for the shorter bridge, and about 260 km/h for the longer one. A peak values of deflection and the longitudinal stress is more noticeable for the CB15 bridge. Longitudinal tension stress reach similar values in both cases for velocities beyond the range close to the resonant velocity.

Acknowledgements

Thanks are due to Prof. Marian Klasztorny from the Department of Mechanics & Applied Computer Science at the Military University of Technology for his guidance, comments and constant support.

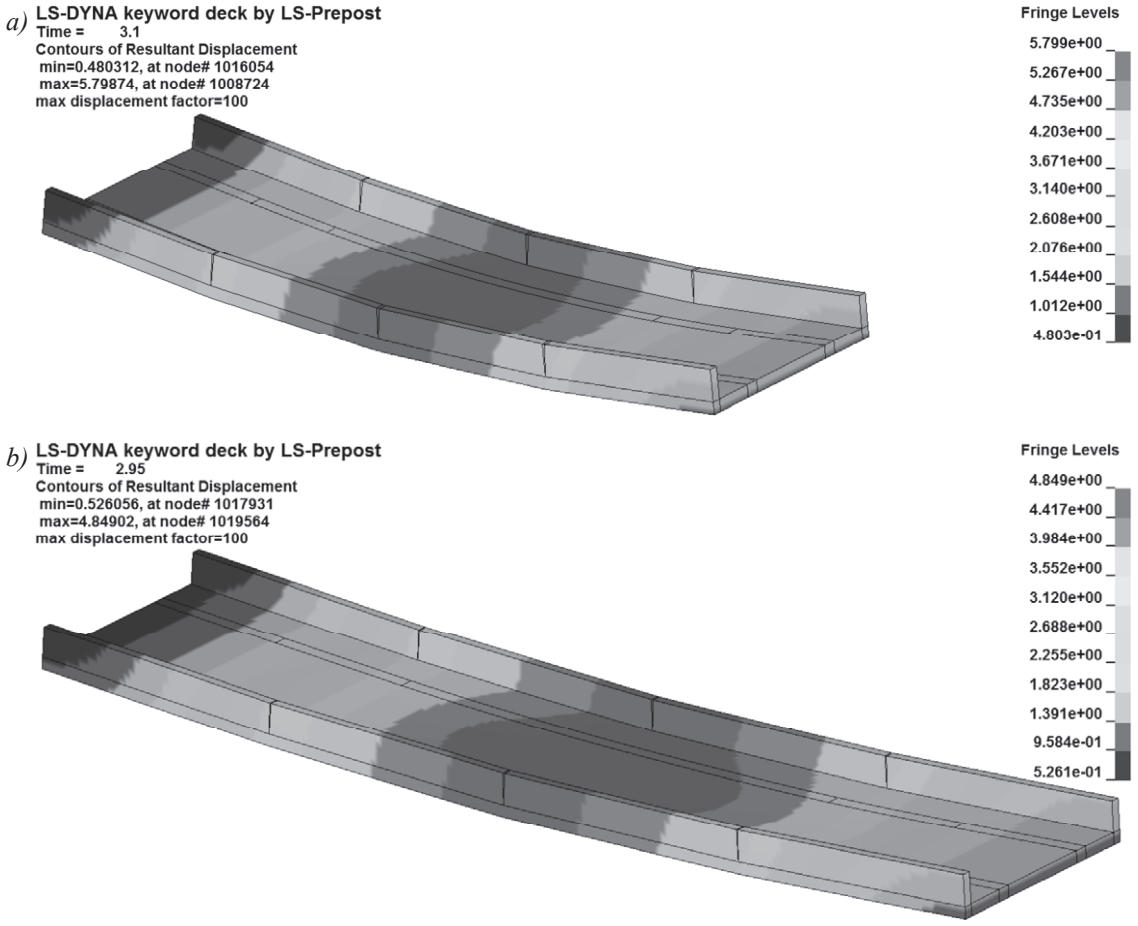

Fig. 10. Contours of resultant displacement for selected moment of time. The results for resonant velocities, correspond to the CB15 (a) and CB21 (b) bridge

References

[1] *First Class Bogies, The Complete Programme for High-Quality Railway Transportation*, Siemens Transportation Systems, http://www.siemens.com/mobility.

[2] Hallquist, J. O., *LS-DYNA V971 R4 Beta. Keyword User's Manual*, LSTC Co., Livermore, CA, United States 2009.

[3] *High Speed Trainset Velaro E for Spanish National Railways RENFE*, Siemens Transportation Systems, http://www.siemens.com/mobility.

[4] http://kolej.krb.com.pl/dt/zal1.htm.

[5] Jones, R. M., *Mechanics of Composite Materials*, Taylor & Francis, London 1999.

[6] Klasztorny, M., *Dynamics of Beam Bridges Loaded by High-Speed Trains* [in Polish], WNT, Warsaw, Poland 2005.

[7] Klasztorny, M., *Vibrations of Single-Track Railway Bridges Under High-Speed Trains* [in Polish], Wroclaw University of Technology Press, Wroclaw, Poland 1987.

[8] Matsuura, A., *Dynamic Behavior of Bridge Girder for High Speed Railway Bridge*, RTRI Quarterly Reports, Vol. 20, Iss. 2, pp. 70–76, 1979.

[9] Niemierko, A., et al., *Reinforcing the Track and the Subgrade in the Approach Zones to Engineering Objects* [in Polish], Project No. M1-123, Research Institute for Roads and Bridges, Warsaw, Poland 2009.

[10] Polish Standard: PN-H-84027-07:1984. *Steel for Rail-Engineering. Normal Rails. Sorts* [in Polish], PKN, Warsaw, Poland 1984.

[11] Steimel, A., *Electric Traction – Motion Power and Energy Supply: Basics and Practical Experience*, Oldenbourg Industrieverlag GmbH, 2007.